Z. Phys. B - Condensed Matter 84, 315-325 (1991)

Condensed
Zeitschrift für Physik B Matter

Tunneling in a periodically driven bistable system

Frank Großmann, Peter Jung, Thomas Dittrich, and Peter Hänggi

Institut für Physik der Universität, Memminger Strasse 6, W-8900 Augsburg, Federal Republic of Germany

Received January 30, 1991

The influence of periodic driving on coherent tunneling is investigated, using a quartic double-well potential in a monochromatic external field as a working example. Extensive numerical studies of the long-time behaviour of this system are combined with an analytical description on basis of the quasienergy formalism. Approximate solutions of the dynamics are possible in the two opposite limits of adiabatic and fast driving, respectively. In both cases, the tunneling rate is enhanced, compared with the unperturbed value. This is confirmed by our numerical results. For driving frequencies in the range of the bare tunnel splitting novel types of tunneling behaviour occur, including *localization* of the wave packet in one of the wells *(coherent destruction of tunneling)*. They can be explained in terms of the local Floquet spectrum and are verified by the time evolution of quantum probabilities.

1. Introduction

The application of periodic external forces to classical and quantum mechanical systems generates a variety of complex behaviour and often produces phenomena completely unexpected from the corresponding undriven dynamics. For example, in one-dimensional nonlinear Hamiltonian systems, periodic driving can lead to chaotic motion which is excluded in their nondriven counterparts [1-4].

In the present paper we investigate the influence of periodic driving on tunneling. Thereby, we restrict ourselves to the regime of zero temperature and vanishing dissipation. Quantum dynamics in the presence of periodic forcing characterizes the physics of a wide class of systems, including, e.g., atoms or molecules exposed to laser fields [5-9] and microwave irradiated Josephson junctions [10]. Earlier theoretical work on driven quantum systems in metastable and scattering situations uses semiclassical-like approximations [11-13], or is based on a semiclassical two-level treatment [14]. In a recent paper [15], Lin and Ballentine represent calculations of quasi-probability distributions for periodically driven double-well potentials in the context of a chaos transition in the corresponding classical problem.

As an archetypal model system, we study the quantum dynamics of a particle in a quartic double-well potential

$$V_0(x) = -\frac{a}{2}x^2 + \frac{b}{4}x^4 \quad a, b > 0, \tag{1}$$

perturbed by a periodic monochromatic signal (no kick-type perturbation!), i.e.,

$$V(x,t) = V_0(x) + xS\sin\omega t. \tag{2}$$

The corresponding classical problem has been studied extensively in [2]. The quantum dynamics in the deep quantal regime, however, has not been addressed up to now. Clearly, our study has been motivated by the problem of tunneling in multistable potentials in presence of time-periodic forces.

In the present work, we combine analytical arguments, using the Floquet formalism, with extensive numerical studies to access the regimes far from the classical limit and of strong forcing at arbitrary frequency. In this way, we not only obtain information on the influence of the forcing on well-known quantities such as the tunneling frequency, but find novel coherence phenomena which challenge the traditional view of tunneling.

In Sect. 2 we review the phenomenon of tunneling in the stationary case with an emphasis on the semiclassical evaluation of the tunneling frequency. Section 3 is the central part of this paper as it contains our approach to tunneling in the presence of external periodic forces. In Sect. 3.1 we explain the relevance of the quasienergies for tunneling. Additionally, in Sect. 3.2, the *local* quasienergy spectrum is shown to play a major role. In the following subsections we will present our results. The numerical calculation of quasienergies is based on a matrix-continued fraction method. These quantities will be compared with the local spectrum determined from the time evo-

lution of a suitably chosen initial wave packet. In Sects. 3.3 and 3.4, two limiting cases are discussed: both for very low and very high external frequencies, we contrast our approximate theoretical results with the numerical ones. Section 3.5 covers the interesting regime of intermediate driving frequencies, in the near of the fundamental resonance at $\omega \approx \sqrt{2a}$. We present numerical results with some intriguing conclusions concerning the notion of tunneling. In Sect. 3.6, we introduce and discuss a surprising effect which occurs at external driving frequencies near the unperturbed tunnel splitting: for suitably chosen external force, tunneling can be almost completely suppressed. Section 4 contains a summary of this work.

2. Tunneling in the double-well potential

In this section we address the unperturbed problem, given by the one-dimensional quartic double-well potential

$$V_0(x) = -\frac{m\omega_0^2}{4} x^2 + \frac{m^2\omega_0^4}{64 E_B} x^4, \tag{3}$$

where m denotes the mass of the particle, ω_0 is the classical frequency of small oscillations at the bottom of each well and E_B denotes the barrier height. For ease of notation we introduce the dimensionless variables

$$\sqrt{\frac{m\omega_0}{\hbar}}\, x \to x, \quad \omega_0 t \to t.$$

The time-dependent Schrödinger equation thus takes the form

$$\mathrm{i}\dot{\Psi}(x,t) = H_0(x)\,\Psi(x,t), \tag{4}$$

with the Hamiltonian

$$H_0(x) = -\tfrac{1}{2}\partial_x^2 - \tfrac{1}{4}x^2 + \frac{1}{64 D} x^4. \tag{5}$$

Thereby we have introduced the dimensionless barrier height $D = E_B/\hbar\omega_0$. Note that as a consequence of the scaling of variables energies are measured in units of $\hbar\omega_0$.

As noted first by Friedrich Hund in 1927 [16], quantum mechanics implies coherent tunneling of the particle from one well to the other. The oscillation frequency can be calculated by considering the time evolution of a wave function initially centered in one of the wells. The two energy eigenfunctions ψ_1, ψ_2, corresponding to the two lowest energy levels E_1, E_2, are approximately given by the symmetric and antisymmetric superpositions, respectively, of the ground states in the two wells for infinite barrier height. Consequently, an eigenstate localized, say, in the left well is given by

$$\Psi_L(x,0) = \frac{1}{\sqrt{2}}\,[\psi_1(x) + \psi_2(x)]. \tag{6}$$

Table 1. Numerically versus semiclassically calculated tunnel splittings for $S=0$ and different values of the barrier height D in units of $\hbar\omega_0$

D	Δ	Δ_s
1	0.0239229	0.0308172
1.5	0.0022620	0.0026225
2	0.0001895	0.0002104
2.5	0.0000151	0.0000163

The time evolution of the absolute square of (6) reads

$$|\Psi_L(x,t)|^2 = \tfrac{1}{2}\{|\psi_1(x)|^2 + |\psi_2(x)|^2 + 2|\psi_1(x)\,\psi_2^*(x)|\cos(E_2 - E_1)\,t\}, \tag{7}$$

which reveals that the tunneling frequency corresponds to the difference of the two lowest energy levels of the potential. It is usually referred to as the tunnel splitting $\Delta = E_2 - E_1$.

The exact eigenvalues of the corresponding stationary Schrödinger equation cannot be calculated analytically. Nevertheless, semiclassical calculations of the tunnel splitting exist. Using path integral methods [17], one finds

$$\Delta_s = 8\sqrt{\frac{2D}{\pi}}\exp\left(-\frac{16D}{3}\right) \tag{8}$$

for the tunnel splitting, where the subscript s indicates that this is a semiclassical result. In Table 1, numerical results for Δ, obtained by using a matrix-continued-fraction method (see the Appendix), are compared with the semiclassical prediction.

The deviation of the semiclassical results from the exact numerical ones decreases from approximately 29% ($D=1$) to 8% ($D=2.5$). This is consistent with the fact that for this problem the semiclassical limit corresponds to $D \to \infty$. For the decay rate out of the lowest state of a metastable system, such as a cubic potential, an analogous comparison leads to similar findings [18].

3. The driven double-well potential

In this section we discuss quantum tunneling in the presence of an external periodic disturbance. For the solution of the time-dependent Schrödinger equation we apply the Floquet formalism, which is based on the discrete time-translation symmetry of the Hamiltonian. This allows to make use of analogies between the unperturbed and the periodically driven case.

3.1. *Floquet formalism*

In the following we will consider the time-dependent potential (2), that describes the coupling of the double-well system to an external monochromatic force field.

Introducing the dimensionless force strength

$$\frac{1}{\sqrt{\hbar m \omega_0^3}} S \to S,$$

the Hamiltonian reads

$$H(x,t) = H_0(x) + xS \sin wt, \tag{9}$$

with $w = \omega/\omega_0$ denoting the ratio of the external frequency to the frequency of small oscillations at the bottom of each well. Using the periodicity of the Hamiltonian, the Floquet theorem [19] states that a solution of the time-dependent Schrödinger equation

$$\mathrm{i}\dot{\Psi}(x,t) = H(x,t)\,\Psi(x,t) \tag{10}$$

can be factorized as

$$\Psi_k(x,t) = \exp\{-\mathrm{i}\varepsilon_k t\}\,\Phi_k(x,t),$$
$$\Phi_k(x,t) = \Phi_k(x,t+T), \tag{11}$$

where Φ_k are the time-periodic Floquet functions, and the quantities ε_k are referred to as *quasienergies* [6, 19] in the following.

There exist only very few driven quantum systems which are analytically solvable. One of them is the periodically driven stable harmonic oscillator [20]. For the problem posed in this paper, however, we have to rely on numerical methods. The method we employ to determine the quasienergies can be used for any confining nonlinear driven system and is given in the Appendix. Note that for this type of problems the quasienergies are real quantities. This follows from the fact that the Hamilton operator $\mathscr{H} = H(x,t) - \mathrm{i}\partial_t$ is Hermitian in an extended Hilbert space [21], made up from the direct product of the space of all square integrable functions on configuration space with the space of square integrable periodic functions in time. Taking into account the factorization of Ψ in (11), we see that the quasienergies are analogous to the energies in the stationary case.

At this point we mention an interesting property of the Floquet solution. From the factorization in (11) it is obvious that

$$\Phi_{k,l}(x,t) \equiv \Phi_k(x,t)\exp(\mathrm{i}lwt),$$
$$\varepsilon_{k,l} \equiv \varepsilon_k + lw, \quad l = 0, \pm 1, \pm 2, \ldots, \tag{12}$$

represents the same total solution as in (11), i.e.

$$\Psi_k(x,t) = \exp\{-\mathrm{i}\varepsilon_{k,l} t\}\,\Phi_{k,l}(x,t). \tag{13}$$

The index k corresponds to the quantum number in the undriven case. One value of k now defines a whole *class* of Floquet functions, because every l yields the same total solution. The quasienergies are thus only defined modulo w.

This provides a clue concerning the behaviour of quasienergies under the variation of external parameters [22]. To this end we investigate the effect of the generalized parity transformation P, defined by

$$x \to -x, \quad t \to t + \frac{\pi}{w}.$$

$\mathscr{H}$ is invariant under the transformation P. This implies that the Floquet functions must transform according to

$$P\Phi_{k,l}(x,t) = \pm \Phi_{k,l}(x,t). \tag{14}$$

The notion of parity is thus extended to the periodically driven case. From (12) it is obvious that two Floquet functions, $\Phi_{k,l}$, $\Phi_{k',l'}$, have the same or different parities according to the difference $(k-l)-(k'-l')$ being even or odd, respectively.

There are some features of the parameter dependence $\varepsilon_{k,l}(S,w)$ which deserve special mention. In the limit $S \to 0$ of vanishing amplitude of the driving force, the remaining w-dependence takes a particularly simple form,

$$\varepsilon_{k,l}(0,w) = E_k + lw, \tag{15}$$

where E_k is the k-th unperturbed level. Equation (15) implies that there is an infinite number of resonances $\varepsilon_{k,l}(0,w) = \varepsilon_{k',l'}(0,w)$ at driving frequencies

$$w_{k,l;k',l'} = \frac{E_k - E_{k'}}{l' - l}. \tag{16}$$

In a quantum-optical context, they can be interpreted as $l'-l$-photon transitions.

At finite force amplitudes, $S \neq 0$, the linear law (15) looses its exact validity. The deviation becomes particularly large in the vicinity of a subset of the resonances, given by (16): if the corresponding eigenstates $\Phi_{k,l}$, $\Phi_{k',l'}$ belong to the same parity class, these intersections become avoided crossings. Due to their smallness and high density in parts of parameter space, the occurrence of avoided crossings along a one-dimensional section of a quasienergy surface often makes it practically impossible to trace it back to the unperturbed value E_k from which it emerges. Therefore, in many cases, a quasienergy spectrum obtained numerically cannot be labeled reliably, and the parities of the corresponding Floquet functions have to be inferred indirectly.

Both exact and avoided crossings show up in the time domain in a conspicuous way: they translate into diverging or extremely long time scales, respectively, in the evolution of a wave packet. In the subsequent sections, we shall briefly introduce the formal tools that establish the relationship between Floquet spectrum and long-time behaviour, and then illustrate its usefulness in the present context by several numerical examples.

3.2. *Staying probability and local spectrum*

For the undriven double-well potential, it was shown in Sect. 2 that the tunneling frequency is given by the splitting between the two lowest-lying energy eigenvalues. In the driven case, it is necessary to generalize this relation on basis of the concept of quasienergies. This is straightforward in the two opposite limits of very slow (adiabatic) and very fast driving frequency: here the separation of time scales implies that the structure of the Floquet spec-

trum deviates only slightly from that of the energy spectrum in the undriven case. Consequently, the difference between the two quasienergies corresponding to the lowest-lying energy eigenvalues still plays the role of the tunneling frequency. For intermediate driving frequencies, however, the Floquet spectrum may loose any resemblance to the unperturbed case, and the simple oscillation of probability between the two wells is replaced, in general, by a more complicated dynamics.

The relation between this time evolution and properties of the Floquet spectrum can be made precise using the concepts of the probability to stay and of the local spectrum [23, 24]. In order to set the stage for the subsequent discussion of our numerical results, we now briefly introduce these concepts.

The probability to stay in the initial state after n periods $T=\frac{2\pi}{w}$ of the external field is given by

$$P(n)=|\langle\Psi(nT)|\Psi(0)\rangle|^2, \quad n=1, 2,\ldots. \tag{17}$$

This absolute square of the overlap of a wave function propagated in time with its initial state is in the literature also referred to as non-decay probability, survival probability, or autocorrelation function. Expanding both $|\Psi(0)\rangle$ and $|\Psi(nT)\rangle$ in the Floquet basis and using Eq. (11) to express their time evolution, we find

$$\begin{aligned} P(n)&=\sum_{\alpha,\beta}\exp\{\mathrm{i}(\varepsilon_\alpha-\varepsilon_\beta)nT\} \\ &\quad\times|\langle\Phi_\alpha|\Psi(0)\rangle|^2\,|\langle\Phi_\beta|\Psi(0)\rangle|^2 \\ &=\xi^{-1}+\sum_{\alpha\neq\beta}\exp\{\mathrm{i}(\varepsilon_\alpha-\varepsilon_\beta)nT\} \\ &\quad\times|\langle\Phi_\alpha|\Psi(0)\rangle|^2\,|\langle\Phi_\beta|\Psi(0)\rangle|^2, \end{aligned} \tag{18}$$

where the index α refers to pairs k, l, with $k=1, 2, 3\ldots$ and a single value of l chosen such that $-\pi\leqq\varepsilon_{k,l}T<\pi$ (correspondingly for β). Additionally, the abbreviation

$$\begin{aligned} \xi^{-1}&=\sum_\alpha|\langle\Phi_\alpha|\Psi(0)\rangle|^4 \\ &=\lim_{N\to\infty}\frac{1}{N}\sum_{n=0}^{N-1}P(n) \end{aligned} \tag{19}$$

has been used for the long-time average of $P(n)$. Equation (18) shows that the time evolution of this characteristic dynamical quantity is determined by the differences of those quasienergies which correspond to eigenstates overlapping appreciably with the initial state. For the special case of a driven double-well system, the probability to stay may be used as a crude, but simple diagnostic to assess the tunneling phenomenon, if the initial state is chosen, e.g., as a Gaussian wave packet centered in one of the wells.

Consequently, in the energy domain, the relevant quantity for the description of tunneling is not the unbiased Floquet spectrum but the local spectrum. Its density is defined by endowing each eigenvalue with a weight equal to the overlap of the corresponding eigenstate with an adequately chosen reference state,

$$P_1^{\mathrm{loc}}(\eta)=\sum_\alpha|\langle\Phi_\alpha|\Psi\rangle|^2\delta(\eta-\varepsilon_\alpha T), \tag{20}$$

where it is understood that the δ-function is 2π-periodic.

As a straightforward generalization of (20), the definition of the local spectral two-point correlation function reads [24]

$$\begin{aligned} P_2^{\mathrm{loc}}(\eta)=\int_0^{2\pi}\mathrm{d}\Omega\sum_{\alpha\neq\beta}&|\langle\Phi_\alpha|\Psi\rangle|^2\,|\langle\Phi_\beta|\Psi\rangle|^2 \\ &\times\delta\left(\Omega+\frac{\eta}{2}-\varepsilon_\alpha T\right)\delta\left(\Omega-\frac{\eta}{2}-\varepsilon_\beta T\right). \end{aligned} \tag{21}$$

An averaging over the mean position Ω of the two quasienergies involved is implicit in this definition.

The local spectral correlation function (21) is related by Fourier transform to the probability to stay, (18) [24],

$$P_2^{\mathrm{loc}}(\eta)=\frac{1}{2\pi}\sum_{n=-\infty}^{\infty}\exp\{-\mathrm{i}\eta n\}(P(n)-\xi^{-1}). \tag{22}$$

Summarizing the preceeding formal arguments, we conclude that the concept of tunneling has to be replaced, in the driven double-well system, by the *time evolution of the staying probability for a wave packet initially centered in one of the wells.* This dynamical quantity, in turn, is adequately analyzed in terms of the local spectrum and its two-point correlation function, with that initial state serving as the reference state.

These considerations serve as a guide how to investigate the long-time behaviour of a wave packet initially centered in the left well and subject to a periodic external force with a frequency higher than the unperturbed tunneling frequency. This will be done using the notion of quantum maps [25]. Because of the periodicity of the Hamiltonian (9), the propagator has the property

$$U(nT)=U^n(T), \tag{23}$$

indicating an elegant way to obtain the long-time behaviour of a periodically driven quantum system in a stroboscopic fashion: to this end we construct the propagator over one period of the external force by solving the time-dependent Schrödinger equation numerically. This propagator is then applied iteratively to a Gaussian wave packet

$$|\Psi_{\mathrm{in}}(0)\rangle=\sum_m c_m|\gamma_m\rangle. \tag{24}$$

Here $|\gamma_n\rangle$ are harmonic-oscillator eigenfunctions, given in coordinate representation in the Appendix (A4), and the weighting factors c_m are Poisson distributed, in a way that the particle will initially be centered in the left well. By this procedure we obtain the time evolution of the probability to stay. From the time series $P(n)$, a discrete Fourier transform can be calculated, allowing us to determine the frequencies relevant for tunneling (cf. (22)) and to compare them with the corresponding quasienergies.

Before going to the topic of complex interference phenomena at intermediate driving frequencies, we will now consider the two limiting cases of adiabatic and high-frequency driving. Here, analytical approximations are still possible, and serve to check theory and numerics against each other.

3.3. *Adiabatic limit*

When we prepare a particle in a superposition of the Floquet functions corresponding to the wave functions of the two lowest unperturbed eigenvalues E_1, E_2, the time evolution of the absolute square of this function is

$$\begin{aligned}&\tfrac{1}{2}|\Psi_1(x,t)+\Psi_2(x,t)|^2\\&=\tfrac{1}{2}\{|\Phi_{1,0}(x,t)|^2+|\Phi_{2,0}(x,t)|^2\\&\quad+2|\Phi_{1,0}(x,t)\,\Phi^*_{2,0}(x,t)|\\&\quad\times\cos[(\varepsilon_{2,0}-\varepsilon_{1,0})t-\varphi(x,t)]\},\end{aligned}\tag{25}$$

where $\varphi(x,t)$ is the time periodic phase of $\Phi_{1,0}(x,t)\,\Phi^*_{2,0}(x,t)$. For external forces varying slowly compared to the time scale given by the difference of the two quasienergies, the Floquet functions are quasistationary so that this difference obviously plays the role of a tunneling frequency.

Adiabatic approximation. In the adiabatic case, the frequency of the external force must be small compared with the smallest internal frequency, given by the unperturbed tunneling frequency. Therefore, in the adiabatic limit, we assume $w \ll \Delta$.

What happens, when a weak and sufficiently slow external force perturbs the system? Because of the x-dependence of the slowly varying time periodic potential (9), the fast oscillating wave packet will see a stationary distorted potential during one period of tunneling. For asymmetric double-well potentials, we can calculate the tunnel splitting in the semiclassical limit from its value Δ for the symmetric potential and the asymmetry σ, by using

$$\Delta_\sigma = \sqrt{\Delta^2+\sigma^2}. \tag{26}$$

This formula certainly holds if $\sigma \ll 1$, i.e., if the distortion is much smaller than the lowest energy eigenvalue at the bottom of one well. With this restriction, σ may range from 0 to values large compared to Δ.

We now have to average Δ_σ over one period of the external force to find the tunnel splitting in the adiabatic case. From the Hamiltonian (9) of the driven double-well we get

$$\sigma = \sqrt{32D}\, S \sin\phi\,, \tag{27}$$

where ϕ is the phase of the slowly varying external force. Averaging equation (26) over one period of $\sin\phi$ then leads to

$$\Delta_{\mathrm{ad}} = \frac{2\Delta}{\pi}(1+\alpha)^{1/2} E\left(\sqrt{\frac{\alpha}{1+\alpha}}\right) \tag{28}$$

for the estimated adiabatic tunnel splitting. Here $E(x)$ denotes the complete elliptic integral [26], and we used the abbreviation

$$\alpha = \frac{32 S^2 D}{\Delta^2}. \tag{29}$$

An expansion of the right-hand side of (28) in the limits $\alpha \ll 1$, and $\alpha \gg 1$, reveals that

$$\Delta_{\mathrm{ad}} \xrightarrow{\alpha \ll 1} \Delta\left(1+\tfrac{1}{4}\alpha\right), \tag{30}$$

$$\Delta_{\mathrm{ad}} \xrightarrow{\alpha \gg 1} \frac{8\sqrt{2D}}{\pi} S, \tag{31}$$

respectively. This predicts that the averaged adiabatic tunnel splitting increases quadratically for small S and approaches a linear dependence for large S. Furthermore, it implies an enhancement of tunneling for arbitrary external force in the adiabatic case.

Numerical results. For frequencies small compared to the undriven tunnel splitting, we have evaluated the quasienergy difference, $\varepsilon_{2,0}-\varepsilon_{1,0}$, for the driven double-well potential for several values of the external field strength. In all our investigations the amplitude of the external force has been chosen sufficiently small so that the potential remains bistable. The outcome for small frequencies does not depend on the external frequency up to

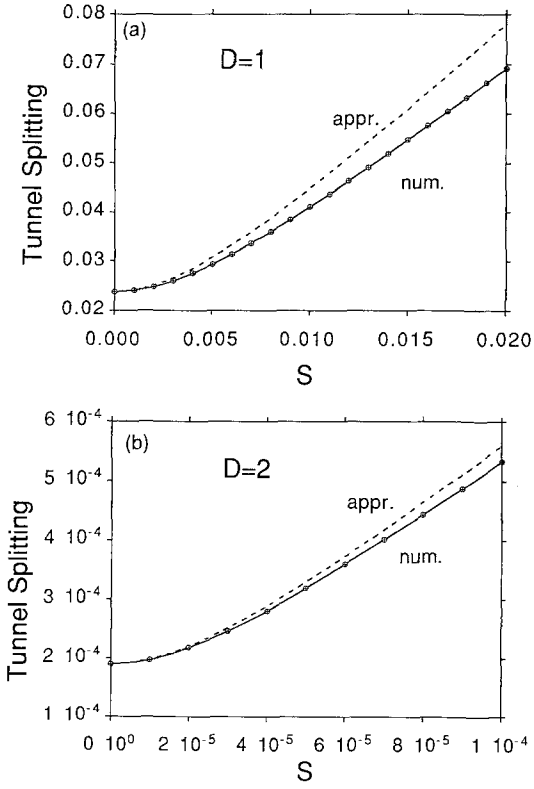

Fig. 1. Dimensionless tunnel splitting Δ_{ad} of the driven double well, in the cases **a** $D=1$, $w=10^{-4}$, **b** $D=2$, $w=10^{-6}$, as a function of the external force strength; appr.: denotes adiabatic approximation, num.: denotes numerically calculated quasienergy difference $\varepsilon_{2,0}-\varepsilon_{1,0}$

$w \sim \frac{\Delta}{10}$. In Fig. 1a, b, the difference of the two quasienergies emerging from the lowest stationary energies as calculated numerically and the adiabatic approximation for the tunnel splitting are plotted versus the field strength. The outcome exhibits the predicted behaviour. The quasienergy differences plotted in Fig. 1, taken modulo w, are playing the role of a tunneling frequency in a stroboscopic dynamics of the tunneling process.

We did the calculations for two different values of the barrier height. In both cases, the values predicted by the semiclassical approximation exceed the numerical results. This is due to the effective softening of the potential towards the top of the barrier. The conditions for the validity of the semiclassical approximation are thus better fulfilled for the case of a higher barrier. So the discrepancy between the numerically evaluated and the theoretically predicted curve is smaller in the case $D=2$, compared to $D=1$. This is obvious from a comparison between Fig. 1a and b.

3.4. *High-frequency limit*

The idea of our high-frequency approximation is to assume that the external force varies so rapidly ($w \gg 1$) that the wave function is not able to respond appreciably and thus remains nearly constant over one external period. This assumption is suggested by the behaviour of the driven harmonic oscillator [20] in the same limit. In a sense, the high-frequency case is converse to the adiabatic limit. While, in the latter case, the slow variation of the external force, compared with the lowest system frequency, leads to a separation of the corresponding time scales, the roles of the slow and the fast dynamics are exchanged in the present limit.

High-frequency approximation. To obtain a crude estimate for the frequency dependence of tunneling for rapidly varying external force, we perform the unitary transformation

$$\Psi(x,t) = \exp\left[-\mathrm{i}\frac{S}{w}\cos(wt)\,x\right] g(x,t) \tag{32}$$

in the time-dependent Schrödinger equation (10). To arrive at an equation for $g(x,t)$, we employ a well-known relation for an operator surrounded by exponentials of another operator [27], yielding

$$\mathrm{i}\dot{g}(x,t) = \left\{-\tfrac{1}{2}\partial_x^2 + V(x) - \mathrm{i}\frac{S}{w}\partial_x \cos(wt)\right\} g(x,t). \tag{33}$$

Here, we have dropped x-independent terms because we are only interested in energy differences.

At this point we note that (33) formally resembles the nontransformed Schrödinger equation (10), the only difference being the coupling of the force to *momentum* instead of position. Thus, the unitarity of transformation (32) shows that the Hamiltonian

$$\tilde{H}(x,t) = -\tfrac{1}{2}\partial_x^2 + V(x) - \mathrm{i}\frac{S}{w}\partial_x \cos(wt) \tag{34}$$

is *quasienergy-isospectral* to the Hamiltonian in (9).

Introducing a second transformation

$$g(x,t) = \exp\left[\frac{S}{w^2}\sin(wt)\partial_x\right] f(x,t), \tag{35}$$

which is again unitrary, inserting it into (33), and using the operator relation mentioned above, leads to

$$\mathrm{i}\dot{f}(x,t) = \left\{-\tfrac{1}{2}\partial_x^2 + V\left[x - \frac{S}{w^2}\sin(wt)\right]\right\} f(x,t). \tag{36}$$

Here the argument of the potential is shifted by the external perturbation. To determine the tunnel splitting in the high-frequency case, we average (36) over one external period. This shows that the quantum particle sees an effective potential, given by

$$\bar{V} = -\tfrac{1}{4}x^2\left[1 - \frac{3}{16D}\left(\frac{S}{w^2}\right)^2\right] + \frac{1}{64D}x^4. \tag{37}$$

Again, x-independent shifts of the energy scale are not included. Thus, one particular effect of the high-frequency field on the double-well system, in this approximation, is to lower the barrier height. From (37), it follows that

$$\bar{D} = D\left[1 - \frac{3}{16D}\left(\frac{S}{w^2}\right)^2\right] < D, \tag{38}$$

is the effective barrier-height in the high-frequency case. Thus we can calculate the corresponding tunnel splitting semiclassically from (8).

Here we note another interesting fact by considering the classical Hamiltonian corresponding to the one given in (9). Averaging the corresponding classical equation of motion, using the analogous high-frequency assumptions and quantizing subsequently, yields the same effective potential (37). The classical considerations have been used in [28] to deduce an effective Langevin equation for a Brownian particle in a bistable potential under external forcing at high frequencies.

Since the transformations (32), (35) are unitary, the time evolution of $|f(x,t)|^2$ is identical with that of $|\Psi(x,t)|^2$. With the barrier height from (38), we therefore obtain an estimate for the tunnel splitting in the high-frequency case. The ratio of the semiclassical high-frequency tunnel splitting to its unperturbed value is exponentially enhanced,

$$\frac{\Delta_{s,\mathrm{HF}}}{\Delta_s} \approx \left[1 - \frac{3}{16D}\left(\frac{S}{w^2}\right)^2\right] \exp\left[2\left(\frac{S}{w^2}\right)^2\right] > 1. \tag{39}$$

In the high-frequency case, this quantity is always larger than one and depends on the external parameters solely via the ratio $\frac{S}{w^2}$. For very high frequencies it approaches one, i.e., $\bar{D} \to D$.

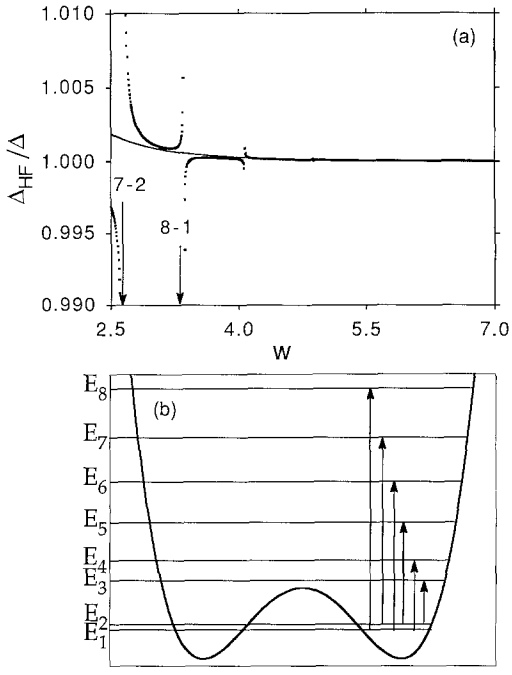

Fig. 2. a Quasienergy difference yielding Δ_{HF} (scaled with respect to the unperturbed tunnel splitting) corresponding to the largest peak in the Fourier spectrum (dots) versus w, for high frequencies. This is compared to the high frequency estimate (solid line) in the case $D=1$, $S=0.2$. The arrows are indicating two of the energy differences depicted in **b**. **b** Energy eigenvalues of the unperturbed double-well potential ($D=1$). Arrows indicating the differences between eigenvalues of different parity

Numerical results. We have determined the quasienergies relevant for tunneling also in the high-frequency case. In Fig. 2a we have plotted the ratio of the driven to the undriven value of the tunnel splitting versus frequency. The numerical results are compared with the high-frequency estimate (39). We observe the predicted limiting behaviour for $w\to\infty$.

At specific external frequencies, however, this behaviour is disrupted. The frequencies for which the system's response deviates from the predicted behaviour correspond to the resonances mentioned in Sect. 3.1 (cf. (16)). They can be associated with differences between unperturbed eigenstates with different parity, as indicated in Fig. 2b. Concerning the Floquet solution, we observe an avoided crossing between two quasienergies belonging to the same parity Floquet function (Fig. 3a). In the region of closest approach of these two quasienergies, the time evolution (see Fig. 3b) of the wave packet is dominated by three frequencies (cf. Fig. 3c) which correspond to the mutual quasienergy differences in Fig. 3a. Therefore, in the neighborhood of these resonances, tunneling can no longer be characterized by a single frequency. The tunnel splittings Δ_{HF}, we plotted in Fig. 2a are those, corresponding to the highest relevant peaks in the Fourier spectrum.

In the frequency range between the resonances, however, we observe only one dominant peak in the Fourier spectrum of the probability to stay. In these regions, we can approximately describe the time evolution by a single tunnel-splitting Δ_{HF}. Note that for external frequencies higher than $w\approx 5$, the numerical values agree within line thickness with the estimate in (39).

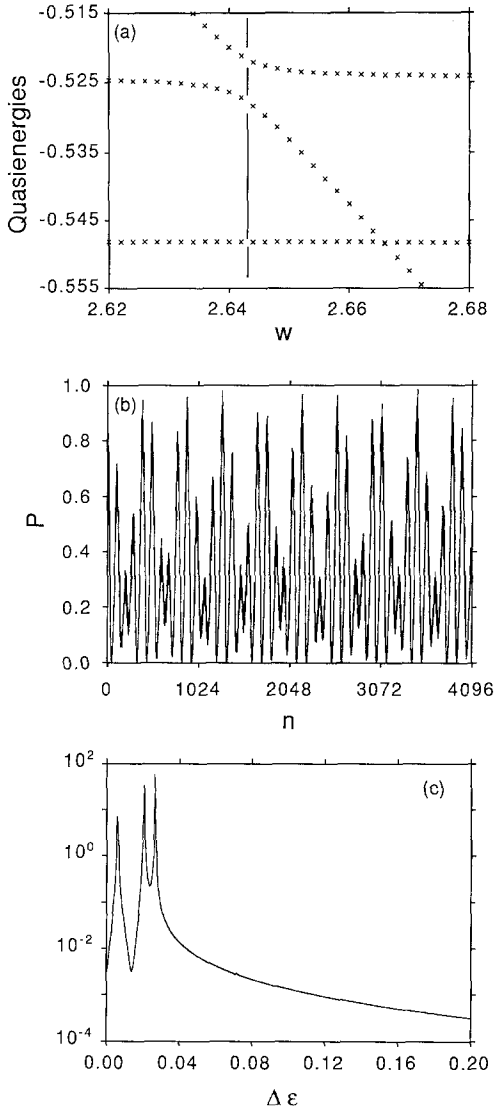

Fig. 3a–c. Investigation of the time scales for tunneling in the driven double well for $D=1$, $S=0.2$, in the vicinity of the fifth resonance (E_7-E_2). **a** Quasienergies versus external frequency w; the vertical line indicates the value of w for the time evolution in **b**. **b** Time evolution of the probability to stay over 2^{12} periods of the external force in the case $w=2.643$. **c** Logarithmic plot of the Fourier spectrum of the time evolution in **b**; ordinate in arbitrary units

3.5. *The fundamental resonance*

In this subsection we will investigate the time evolution of a wave packet initially centered in the left well, when it is subject to external monochromatic forces with frequencies in the vicinity of the difference E_3-E_2, which will be called the fundamental resonance. For $D=1$, it occurs at $w\approx 0.6185$.

Here, even for moderate values of the external field strength, we find marked deviations of the quasienergies from the stationary energy eigenvalues (Fig. 4a). The analysis of the time evolution of the probability to stay (Fig. 4b) shows that, similar to the resonances in the high-frequency case, three frequencies, corresponding to the mutual quasienergy differences in Fig. 4a, are again involved in the tunneling process (Fig. 4c). The largest of these frequencies supersedes the unperturbed tunnel splitting by more than 20%.

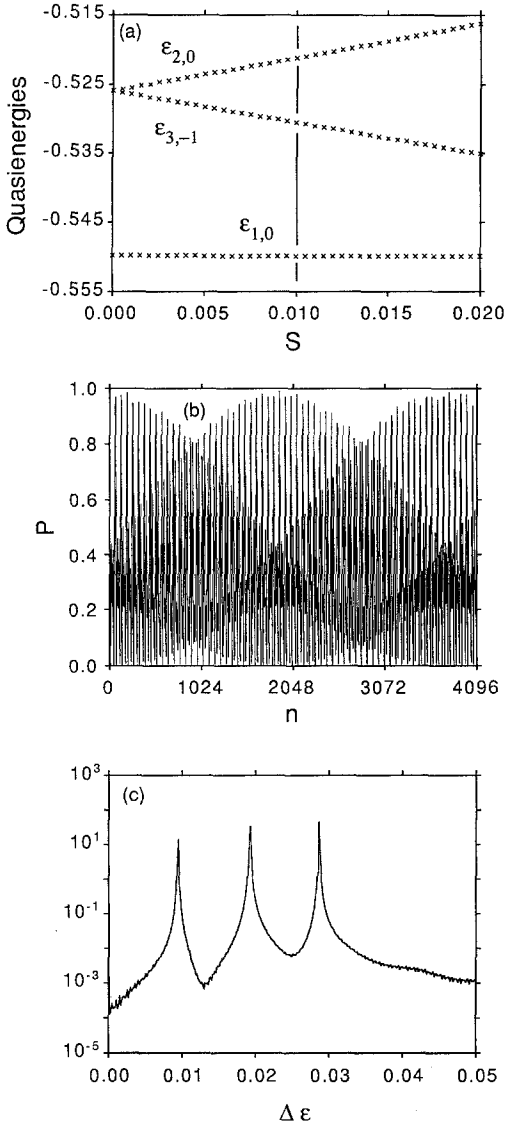

Fig. 4a–c. Investigation of the time scales for tunneling in the driven double well for $D=1$, $w=0.6185$ (fundamental resonance, E_3-E_2). **a** Quasienergies versus external field strength; vertical line indicating the value of S for **b**. **b** Time evolution of the probability to stay over 2^{12} periods of the external force in the case $S=0.01$. **c** Logarithmic plot of the Fourier spectrum of the time evolution in **b**; ordinate in arbitrary units

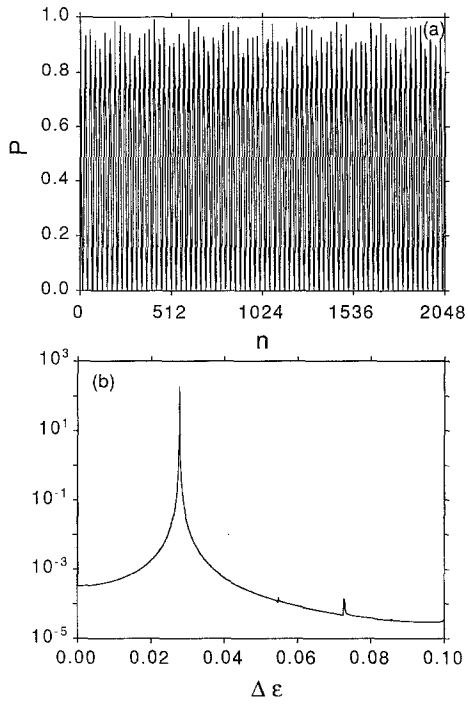

Fig. 5a, b. Investigation of the time scales for tunneling in the driven double well for $D=1$, $w=0.77$ (between the fundamental and the second resonance). **a** Time evolution of the probability to stay over 2^{11} periods of the external force in the case $S=0.05$. **b** Logarithmic plot of the Fourier spectrum of the time evolution in **a**; ordinate in arbitrary units

In the frequency region between the fundamental and the second resonance ($w=E_4-E_1$), tunneling will be dominated by a single frequency only (Figs. 5a, b). For the choice of parameters made in these figures, the driven tunneling frequency is more than 15% larger than the unperturbed tunnel splitting.

3.6. Coherent destruction of tunneling

A range of external frequencies not investigated up to now is the region between the undriven tunnel splitting and the fundamental resonance, $\Delta < w < E_3-E_2$.

Here the behaviour of the quasienergies emerging from the lowest two unperturbed eigenvalues is conspicuous (Fig. 6a). The $l=0$ branches of the two quasienergies

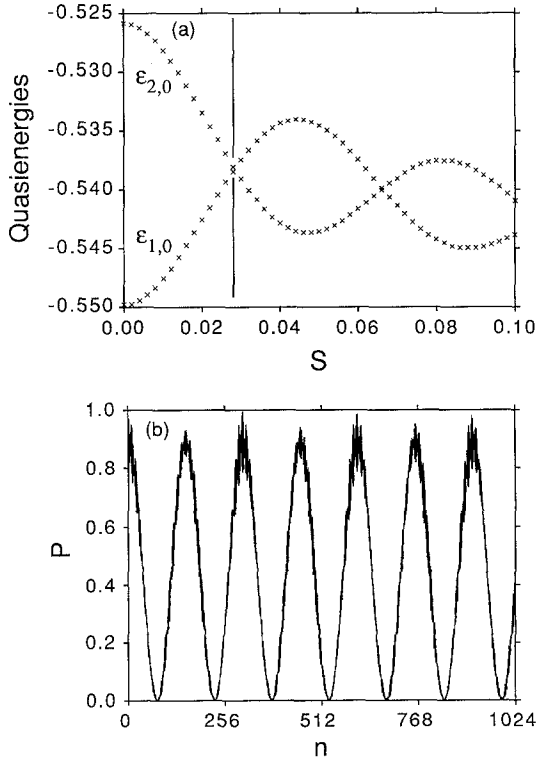

Fig. 6a, b. Investigation of the time scales for tunneling in the driven double-well for $D=1$, $w=0.06$. **a** Quasienergies versus external field strength; vertical line indicating the value of S for **b**. **b** Time evolution of the probability to stay over 2^{10} periods of the external force in the case $S=0.028$

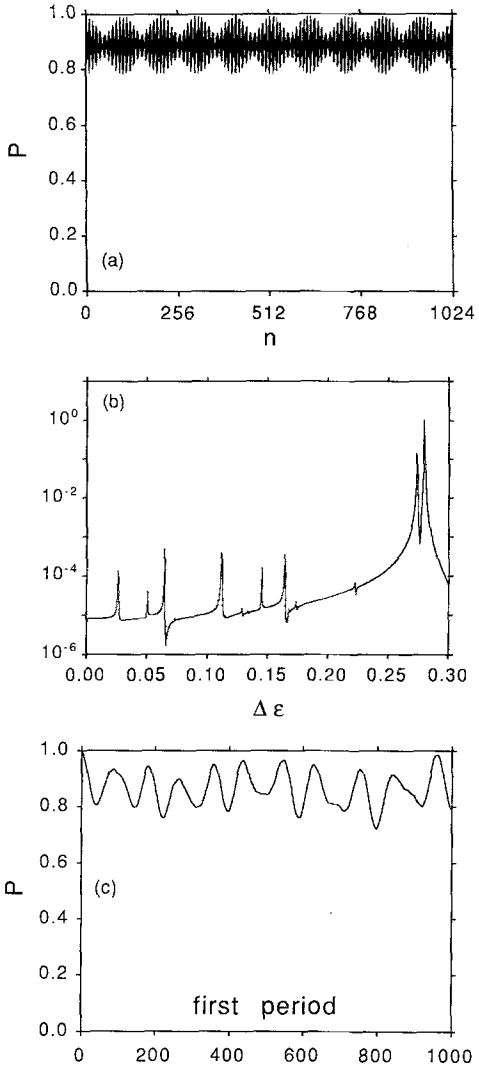

Fig. 7a–c. Suppression of tunneling in the driven double-well for $D=1$, $w=0.06=2.508\,\Delta$. **a** Time evolution of the probability to stay over 2^{10} periods of the external force in the case $S=0.028392$. **b** Logarithmic plot of the Fourier spectrum of the time evolution in Fig. 5a; ordinate in arbitrary units. **c** Time evolution of the probability to stay over the first period of the external force, resolved into 1000 steps

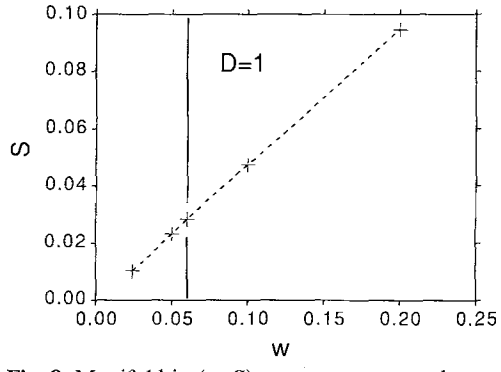

Fig. 8. Manifold in (w, S)-parameter space where an exact crossing of the quasienergies relevant for tunneling occurs for the smallest driving amplitude S (cf. Fig. 6a). The crosses depict numerically verified points in parameter space, where localization occurs. The first cross at $w=0.023922$ corresponds to the bare tunneling frequency, while the third cross (indicated by a vertical line) denotes the parameter set used in Fig. 7

approach each other, cross exactly, deviate and come together again with increasing field strength. These exact crossings have an intriguing consequence: a *suppression* of tunneling in presence of periodic driving.

In Figs. 6b, 7a, we present two typical time evolutions of the probability to stay, with the external parameters tuned into the vicinity of a crossing of the quasienergies. Figure 6b shows that probability is still flowing back and forth between the two wells. The frequency, however, is two orders of magnitude smaller than the unperturbed tunneling frequency, i.e., $\Delta\varepsilon/\Delta \approx 0.016$. Figure 7a depicts the corresponding time evolution, over the same time interval, for a driving force that sits exactly at the crossing, with the best accuracy we could obtain. It shows that the probability to stay remains nearly constant and almost equal to unity, indicating that the wave packet is *localized* in the left well. In the corresponding Fourier spectrum (Fig. 7b), the beating-type behaviour of Fig. 7a translates into a pronounced reduction in weight of the peaks at finite frequencies as compared to Figs. 3c, 4c.

Several remarks are in order. Even for perfect tuning of the parameters of the driving force to the crossing point of the quasienergies, localization is not complete, i.e. a small, periodic deviation of the probability to stay from unity remains. This is due to the fact that the Gaussian wave packet, we prepare as the initial state is not completely exhausted by the two corresponding Floquet states, depicted in Fig. 6a, but has a small, but finite overlap also with other Floquet states. Additionally, we had to make sure that these admixtures and the time evolution of the Floquet functions does not lead to a marked shift of the center of gravity of the wave packet towards the opposite well in the course of a single period of the driving force, which would remain unvisible in the stroboscopic dynamics used here. Figure 7c shows $P(t)$ over the first period of the driving force, resolved into 1000 time steps. We do not observe any high-frequency tunneling obliterated by the discretization of time in Fig. 7a. Finally, we would like to emphasize that the set of parameter values where the two relevant quasienergies cross and, therefore, localization occurs, forms a one-dimensional manifold in (w, S) parameter-space of an approximately linear shape (Fig. 8)! This fact should greatly facilitate an experimental search for the localization phenomenon.

4. Conclusions

We have considered the quantum mechanics of a periodically driven bistable system. In this work, the Floquet formalism has proven an adequate and powerful language to discuss driven tunneling, superior to semiclassical and perturbative techniques. However, it requires to abandon traditional concepts familiar in the field.

In the limits of very low and very fast driving, the separation of time scales allows for an approximate analytical calculation of the quasienergies that correspond to the two lowest energy eigenvalues in the undriven case. Our numerical results confirm that in these limits, their difference can still be interpreted as a tunneling fre-

quency. Its quantitative increase at finite amplitude of the external force indicates that tunneling is enhanced by periodic driving (away from the resonances, cf. Sect. 3.4).

For intermediate frequencies, in general, more than two quasienergies are involved in the dynamics, time evolutions become more complicated and the familiar notion of tunneling is no longer applicable. In this regime, the local quasienergy spectrum and its relationship to characteristic dynamical quantities like the probability to stay provides an adequate formal tool for the interpretation of numerical experiments. Specificially, we observe the slowing down or even divergence of time scales, corresponding to avoided and exact crossings in the quasienergy spectrum, respectively. In particular, for suitably tuned frequency and amplitude of the driving force, coherent tunneling can be suppressed altogether, enabling localization of the wave packet in one of the wells of the bistable potential. An experimental test of this surprising prediction can be carried out with every bistable tunneling system, subject to a monochromatic external field.

This work has been supported by the Deutsche Forschungsgemeinschaft through Grant No. Ha1517/3-1. The help of the staff members of the computer center at the University of Augsburg for providing computer-network facilities is highly appreciated. The numerical calculations have been done on the Cray YMP at the Leibniz-Rechenzentrum, Munich.

A. Numerical calculation of quasienergies

The quasienergies, as was pointed out in Sect. 3, determine the time evolution of the wave function. In order to calculate them, we use a method given by Risken [29] and used by one of us [28] to solve Fokker-Planck equations with periodic drift coefficients. For the treatment of a driven two-level system in this context, see [30].

Dealing with the Schrödinger equation, we expand the Floquet function from (11) in a Fourier series

$$\Phi_{k,l}(x,t)=\sum_{n=-\infty}^{+\infty} c_n^{\varepsilon}(x)\exp(inwt). \tag{A1}$$

The ε-dependence of c_n^{ε} arises because $\Phi_{k,l}$ belongs to the quasienergy $\varepsilon_{k,l}$. Inserting this into the time-dependent Schrödinger equation (10) leads to the recursion relation

$$\left(-\tfrac{1}{2}\partial_x^2-V(x)-\varepsilon+wn\right)c_n^{\varepsilon}(x)$$
$$+\frac{1}{2i}xS[c_{n-1}^{\varepsilon}(x)-c_{n+1}^{\varepsilon}(x)]=0 \tag{A2}$$

for the coefficients $c_n^{\varepsilon}(x)$.

The x-dependence will then be removed by expanding the $c_n^{\varepsilon}(x)$ in the complete orthogonal set of oscillator eigenfunctions,

$$c_n^{\varepsilon}(x)=\sum_{m=0}^{\infty} k_n^m\gamma_m(x), \tag{A3}$$

with

$$\gamma_n(x)=\sqrt{\frac{\alpha}{n!\,2^n\sqrt{\pi}}}\,H_n(\alpha x)\exp(-\tfrac{1}{2}\alpha^2x^2). \tag{A4}$$

Here H_n denote the Hermite polynomials and α is an arbitrary scaling parameter. The ε-dependence of k has not been denoted explicitly. Inserting this expansion in (A2) yields the tridiagonal matrix recursion relation

$$\sum_{m=0}^{\infty} k_n^m G_{j,m}(n)+\sum_{m=0}^{\infty} k_{n+1}^m F_{j,m}^{+}+\sum_{m=0}^{\infty} k_{n-1}^m F_{j,m}^{-}=0. \tag{A5}$$

For arbitrary Hamiltonians one computes the above matrix elements by expressing all powers of x and ∂_x in creation and annihilation operators. For the time-dependent Hamiltonian (5, 9) considered in this paper, the matrices $\mathbf{G}$, $\mathbf{F}^{+}$, $\mathbf{F}^{-}$ are given by

$$\begin{aligned}
G_{j,m}(n)=&-\frac{\alpha^2}{4}\left[\sqrt{(j+2)(j+1)}\,\delta_{j,m-2}\right.\\
&\left.+\sqrt{j(j+1)}\,\delta_{j,m+2}-(2j+1)\,\delta_{j,m}\right]\\
&-\frac{1}{8\alpha^2}\left[\sqrt{(j+2)(j+1)}\,\delta_{j,m-2}\right.\\
&\left.+\sqrt{j(j+1)}\,\delta_{j,m+2}+(2j+1)\,\delta_{j,m}\right]\\
&+\frac{1}{256\,D\alpha^4}\\
&\times\left[\sqrt{(j+4)(j+3)(j+2)(j+1)}\,\delta_{j,m-4}\right.\\
&+\sqrt{j(j-1)(j-2)(j-3)}\,\delta_{j,m+4}\\
&+(4j+6)\sqrt{(j+2)(j+1)}\,\delta_{j,m-2}\\
&+(4j-2)\sqrt{j(j-1)}\,\delta_{j,m+2}\\
&\left.+(6j^2+6j+3)\,\delta_{j,m}\right]-(\varepsilon-wn)\,\delta_{j,m},
\end{aligned}$$

$$F_{j,m}^{\pm}=\pm\frac{iS}{2\sqrt{2}\alpha}\left[\sqrt{j+1}\,\delta_{j,m-1}+\sqrt{j}\,\delta_{j,m+1}\right].$$

The freedom to vary the parameter α can be used to check and to improve the numerics.

To solve Eq. (A5) for the quasienergies, which are explicitly contained in $\mathbf{G}$, we then use a matrix-continued-fraction technique [29].

References

1. Escande, D.F.: Phys. Rep **121**, 165 (1985)
2. Reichl, L.E., Zheng, W.M.: In: Directions in chaos, Vol. 1, Hao Bai-lin (ed.). Singapore: World Scientific 1987
3. Lichtenberg, A.J., Lieberman, M.A.: Regular and stochastic motion. New York: Springer 1981
4. Zaslavsky, G.M.: Phys. Rep. **80**,157 (1981)
5. Blümel, R., Smilansky, U.: Phys. Rev. A**30**, 1040 (1984)
6. Manakov, N.L., Ovsiannikov, V.D., Rapoport, L.P.: Phys. Rep. **141**, 319 (1986)
7. Chu, S.: Adv. Chem. Phys. **73**, 739 (1986)
8. Breuer, H.P., Holthaus, M.: Z. Phys. D – Atoms, Molecules and Clusters **11**, 1 (1989); Phys. Lett. A**140**, 507 (1989)
9. Casati, G., Molinari, L.: Prog. Theor. Phys. [Suppl.] **98**, and references therein
10. Devoret, M.H., Esteve, D., Martinis, J.M., Cleland, A., Clarke, J.: Phys. Rev. B**36**, 58 (1987)
11. Ivlev, B.I., Mel'nikov, V.I.: Phys. Rev. Lett. **55**, 1614 (1985)
12. Fisher, M.P.A.: Phys. Rev. B**37**, 75 (1988)
13. Sokolovski, D.: Phys. Rev. B**37**, 4201 (1988)
14. Sokolovski, S.: Phys. Lett. A**132**, 381 (1988)
15. Lin, W.A., Ballentine, L.E.: Phys. Rev. Lett. **65**, 2927 (1990)
16. Hund, F.: Z. Phys. **43**, 803 (1927)
17. Coleman, S.: In: The whys of subnuclear physics, Proc. of the International School of Subnuclear Physics, Erice, 1977, Zichichi, A. (ed.). New York: Plenum 1979
18. Yaris, R., Bendler, J., Lovett, R.A., Bender, C.M., Fedders, P.A.: Phys. Rev. A**18**, 1816 (1978); Connor, J.N.L., Smith, A.D.: Chem. Phys. Lett. **88**, 554 (1982); Hontscha, W., Hänggi, P., Pollak, E.: Phys. Rev. B**41**, 2210 (1990)
19. Shirley, J.H.: Phys. Rev. **138**, B979 (1965); Zel'dovich, Ya.B.: Zh. Eksp. Teor. Fiz. **51**, 1492 (1966) [Sov. Phys. JETP **24**, 1006 (1967)]; Ritus, V.I.: ibid., 1544 [**24**, 1041 (1967)]
20. ter Haar, D. (ed.): Problems in quantum mechanics, 3rd edn., p. 17. London: Pion 1975; Husimi, K.: Prog. Theor. Phys. **9**, 381 (1953); Kerner, F.H.: Can. J. Phys. **36**, 371 (1958)
21. Sambe, H.: Phys. Rev. A**7**, 2203 (1973)
22. Breuer, H.P., Dietz, K., Holthaus, M.: Z. Phys. D – Atoms, Molecules and Clusters **8**, 349 (1988)
23. Grempel, D.R., Prange, R.E., Fishman, S.: Phys. Rev. A**29**, 1639 (1984)
24. Dittrich, T., Smilansky, U.: Nonlinearity **4**, 59 (1991)
25. Casati, G., Chirikov, B.V., Izrailev, F.M., Ford, J.: In. Casati, G., Ford, J. (eds.) Stochastic behavior in classical and quantum hamiltonian systems. Volta Memorial Conference, Como 1977. Lecture Notes in Physics, Vol. 93. Berlin, Heidelberg, New York: Springer 1979; Berry, M.V., Balazs, N.L., Tabor, M., Voros, A.: Ann. Phys. (N.Y.) **122**, 26 (1979)
26. Gradshteyn, I.S., Ryzhik, I.M.: Table of integrals series and products. New York: Academic Press 1980
27. Wilcox, R.M.: J. Math. Phys. **8**, 962 (1967) Eq. (2.2)
28. Jung, P.: Z. Phys. B – Condensed Matter **76**, 521 (1989)
29. Risken, H.: The Fokker-Planck equation. Springer Series in Synergetics, Vol. 18. Berlin, Heidelberg, New York: Springer 1984
30. Swain, S.: Phys. Lett. A**43**, 229 (1973)